Shear-induced mechanical anisotropy in concentrated emulsions : a Pump Probe Mechanical Spectroscopy study

Nicolas Beyer, Lorry Engel, Pascal Hébraud

Shear-induced mechanical anisotropy in concentrated emulsions : a Pump Probe Mechanical Spectroscopy study†

Nicolas Beyer,[a] Lorry Engel,[a] and Pascal Hébraud*[a]

Received Date
Accepted Date

DOI: 00.0000/xxxxxxxxxx

Concentrated suspensions develop an anisotropic microstructure when subjected to deformation, and this anisotropy persists after flow cessation, leading to direction-dependent mechanical properties. We investigate the mechanical response of a concentrated emulsion following an initial shear deformation. We use a circularly polarized shear to probe the material's elasticity in all directions relative to the initial shear. The emulsion softens along the direction of the applied deformation and stiffens in the perpendicular direction. The degree of mechanical anisotropy is found to depend on the amplitude of the initial deformation, with larger deformations leading to more pronounced directional differences in elasticity.

When subjected to stress, many materials display an elastoplastic response: they deform elastically at small strains, and beyond a certain threshold—the yield strain—they undergo plastic deformation [1]. The plastic regime is characterized by irreversible rearrangements leading to flow. The underlying mechanisms of flow vary depending on the material's structure: in crystalline solids, plasticity deformation typically arises from dislocation motion [2], whereas in amorphous systems, it results from localized structural rearrangements [3–5]. The transition between the elastic and plastic regimes is marked by the yield strain and the corresponding yield stress, both of which depend on the material's prior deformation history [1,6]. Such memory effects, in which the material retains a record of its deformation, are observed in both polycrystalline [7] and amorphous systems [8], though they arise from distinct microscopic mechanisms. In polycrystalline materials, they are linked to the evolution of dislocation networks and grain boundary structures, that encode information about prior loading [6], leading to phenomena such as the Bauschinger effect [8]. In contrast, memory effects in amorphous materials emerge from the rearrangement of local atomic or particle configurations, similarly leading to changes in mechanical properties [9]. In the case of disordered suspensions, these effects have been studied in non-Brownian suspensions. For instance, under cyclic or complex loading, they keep memory of the previously applied deformation amplitudes [10] or directions [10,11] through the formation of stable, non-reversible rearrangements [12,13]. At the particles scale, two situations may be distinguished : interaction between particles that involve friction or adhesion, in which case hysteresis may exist at the scale of contacts between particles, leading to strong anisotropy of the fabric tensor, and of the stress tensor under flow [14]. Moreover, in the case of rough particles, the suspension easily jams under flow [15], and the jammed structure persists for a long time [16]. Conversely, in suspensions of frictionless particles, memory effects must be encoded in the microstructural organization of the suspension at lengths scales larger than the contact between particles. In both cases, stress relaxation in dense suspensions arises from local structural rearrangements induced by applied stress [17,18], which redistribute internal forces in an anisotropic manner [19]. This directional dependence enables the formation of anisotropic microstructures, which in turn give rise to anisotropic mechanical properties. While such behavior has been studied in non-Brownian suspensions [20], the aim of this article is to investigate whether colloidal suspensions at high enough concentration so that thermal rearrangements occur on very long or infinite time scales, can also exhibit mechanical memory.

We study a concentrated suspension of frictionless emulsion droplets and characterize its anisotropic mechanical properties following a previous deformation in the plastic regime. Specifically, we apply a first shear deformation –referred to as the *pump* deformation, by analogy with optical pump-probe spectroscopy – that drives the system into the plastic response regime. Using a home-made bidirectional piezorheometer, that is capable of measuring tangential stresses along any direction relative to the pump shear, we then apply smaller amplitude deformations in the linear regime, or *probe* deformations, to measure the mechanical response at various angles relative to the pump direction. Our results demonstrate that the pump deformation induces an anisotropy in the suspension's mechanical properties. This anisotropy depends both on the suspension's volume fraction and on the specific shear protocol used during the pump

[a] *IPCMS/CNRS, 23 rue du Loess, 67200 Strasbourg, France*
* *pascal.hebraud@ipcms.unistra.fr*
† Supplementary Information available: [details of any supplementary information available should be included here]. See DOI: 10.1039/cXsm00000x/

phase.

1 System and methods

1.1 Emulsions

Dodecane-in-water emulsions are prepared using an ultrasonication method. First, an aqueous solution of 200 mM Sodium Dodecyl Sulfate (SDS) is prepared and pre-mixed with dodecane at a volume fraction of $\phi = 30$ % using a magnetic stirrer. The resulting mixture is then sonicated using a Branson ultrasonicator, yielding an emulsion with an average droplet diameter of approximately 200 nm. To obtain a concentrated emulsion, the sample is centrifuged at 9000 rpm for 40 minutes using an Eppendorf 5804R centrifuge. The clear supernatant is removed, resulting in a concentrated emulsion with a volume fraction of $\phi \approx 72$ %. This concentrated emulsion is then diluted by mixing it with a $\phi = 30$ % emulsion and the volume fraction of each sample is determined from density measurements using an Anton Paar DMA 4500 densitometer. The elastic and loss moduli measured at 10 Hz for a series of such emulsions are plotted in Fig. 1 **(a)**. They exhibit elastic response at small amplitude deformations, with an elastic modulus comprised between 10^3 and 10^4 Pa that increases with the volume fraction. The yield strain defined as the crossing between the elastic and the loss moduli[21] is comprised between 5 and 10 %.

1.2 Pump Probe Mechanical Spectroscopy

We have developed a specific setup to measure the mechanical response of the emulsion along any direction of the shear plane, that is to measure both the velocity/gradient of velocity and the gradient of velocity/rotational of velocity components of the stress tensor. Following the design principles of piezorheometers[22–24], we use piezoelectric devices both to apply the deformation and to measure stresses. The sample is confined between two glass disks, each 40 mm in diameter, with rough surfaces to prevent slip. The spacing and parallelism between the disks are controlled and monitored using capacitive sensors (Micro-Epsilon CSH05FL), with a measurement accuracy better than 1 μm. The attitude of the upper plate is controlled with three micrometer screws. The typical gap between the plates is set to 100 μm. Each disk is attached to a shear piezoelectric actuator (Physik Instrumente 142.10), which enables controlled displacements in both the x and y directions, parallel to the sample plane (see Fig. 1 **(b)**). The bottom piezo stack Π_s acts as the actuator: sinusoidal voltages are independently applied along the x and y axes to generate shear in any desired direction within the $x-y$ plane. While the actuator allows a maximum displacement of 10 μm, typical amplitudes are below 1 μm. The upper stack Π_d, that supports the upper disk, is used as a force sensor : upon stress applied by the sample, it generates charges that are amplified and integrated over time with a home-made charge amplifier, that beahves as a first-order high pass filer with a cut-off frequency equal to 1.7 Hz. This leads to a current, from which, after calibration with PDMS oils of known viscosities, the measurement of stresses applied in any direction on the disk plate, is obtained. In a typical experiment, a sinusoidal shear is applied in any direction, and the x and y components of the induced tangential forces, corresponding to the σ_{zx} and σ_{yz} stress components (see Fig. 1 **(b)**), are measured. Then one may vary the orientation of the applied stress in order to measure the anisotropy of the mechanical response of the system. In this

protocol, the shear γ applied to the system is of the form :

$$\gamma = \left(\gamma_{\parallel}\mathbf{u}_{\parallel} + \gamma_{\perp}\mathbf{u}_{\perp}\right)\cos\omega t \tag{1}$$

where $\mathbf{u}_{\parallel}$ and $\mathbf{u}_{\perp}$ are the directions parallel and normal to the pump shear (detailed below). One measures the stress σ:

$$\sigma = \sigma_{\parallel}\cos(2\pi\nu t + \varphi_{\parallel})\mathbf{u}_{\parallel} + \sigma_{\perp}\sin(2\pi\nu t + \varphi_{\perp})\mathbf{u}_{\perp} \tag{2}$$

from which $\sigma_{\parallel}$, $\sigma_{\perp}$, $\varphi_{\parallel}$ and $\varphi_{\perp}$ may be deduced. Nevertheless, for all samples studied here, we have checked that the response is elastic in all directions, so that the response of the system is fully characterized by the measurement of $\sigma_{\parallel}$ and $\sigma_{\perp}$. This allows to simplify further the sample response measure, by applying a circularly polarized deformation of amplitude γ_0:

$$\gamma = \gamma_0\left(\cos 2\pi\nu t\mathbf{u}_{\parallel} + \sin 2\pi\nu t\mathbf{u}_{\perp}\right) \tag{3}$$

The stress induced by a purely elastic material is of the form

$$\sigma = \sigma_{\parallel}\cos 2\pi\nu t\mathbf{u}_{\parallel} + \sigma_{\perp}\sin 2\pi\nu t\mathbf{u}_{\perp} \tag{4}$$

so that the elastic coefficients $G_{\parallel} = \sigma_{\parallel}/\gamma_0$ and $G_{\perp} = \sigma_{\perp}/\gamma_0$ may be obtained from the large and small axes of the ellipse that represents the parametric plot of σ in the $(\mathbf{u}_{\parallel}, \mathbf{u}_{\perp})$ plane. The mechanical anisotropy of the material may be characterized by its eccentricity, $e = \sqrt{1 - \frac{G_{\parallel}}{G_{\perp}}}$. In a typical measurement, the circularly polarized shear defined by Eq. 3 is applied at frequency $\nu = 10$ Hz and amplitude $\gamma_0 = 3 \cdot 10^{-1}$ %. Initially, the sample is isotropic and therefore its response independent of the orientation of the applied deformation (Fig. 1 **(c)**). The measured elastic modulus is in very good agreement with the elastic modulus measured with a standard rheometer (Fig. 1 **(d)**) : the emulsion exhibits an elastic response at volume fractions larger than ≈ 61 % and the elastic modulus increases with the volume fraction from $\approx 2 \cdot 10^3$ to 10^4 Pa. Notably, the emulsion exhibits an elastic response even at volume fractions below the random close packing concentration, $\phi_{\mathrm{rcp}} = 0.635$, consistent with previous studies[25]. For $\phi > \phi_{\mathrm{rcp}}$, elasticity arises from droplet deformation. In contrast, in the range $\phi_c < \phi < \phi_{\mathrm{rcp}}$, the droplets behave as undeformed hard spheres, and the elasticity arises from entropic origin, characteristic of a colloidal glass[26]. Considering our system, we define $\phi_c = 0.602$ as the volume fraction at which the elastic modulus extrapolates to zero at low ϕ (Fig. 1 **(d)**).

The anisotropy is generated by the application of the pump shear: the bottom stack Π_s is positioned on a translation stage, driven by a large amplitude piezoelectric actuator, that allows displacements comprised between ≈ -60 and 60 μm, corresponding to shear values comprised to -60 and 60 %, along the y-direction. An experiment consists in two successive steps : a pump deformation of amplitude γ_π either in the elastic or in the plastic regime, followed by a probe deformation of amplitude 0.3 % and frequency 10 Hz, at any direction relative to the pump shear. Two different pump protocols are studied : *(i)* constant preshear : the sample is sheared in direction y by a

given value, and left in place. We will refer to this protocol as the "yield protocol", as it intends to study the appearance of anisotropy during start-up flow (Fig. 2 **(a)**); *(ii)* oscillatory deformation: the pump shear consists in a sinusoidal shear at frequency 10 Hz during 5 seconds, after which the sample comes back to the zero deformation state, around which mechanical anisotropy is probed. This will be referred to as the "fatigue protocol" (Fig. 2 **(b)**).

2 Results and discussion

For all studied volume fractions, and for both pump protocols, the elastic modulus as a function of the orientation of the pump/probe angle are well represented by an ellipse (Fig. 2 **(c)** and **(d)**) whose principal axes are parallel and normal to the direction of the pump shear. We now consider the appearance of mechanical anisotropy following each pump protocol.

2.1 Yield protocol

Along the pump direction and at small pump amplitudes γ_π, the elastic modulus $G_\parallel$ increases (Fig. 3 **(a)** top) up to a maximum, whose height, for the lowest concentrated suspension is ≈ 2 % larger than the modulus at rest. Then, the modulus decreases to values smaller than the modulus at rest. The more concentrated the emulsion, the larger the decrease of the modulus. The evolution of the modulus is remarkably different in the direction normal to the pump : for all studied volume fractions, $G_\perp$ increases monotonically with γ_π and, the less concentrated the emulsion, the larger the increase of modulus (Fig. 3 **(a)** bottom). The emulsions thus become softer in the direction parallel to the pump deformation and stiffer in the normal direction. For all studied concentrations, the eccentricity e increases with γ_π and saturates at $e \approx 0.4 - 0.5$ (Fig. 3 **(b)**). We have measured the persistence of this anisotropy over time after the application of the pump deformation, and no decay is observed at least during one hour (Fig. 3 **(b)** *insert*). Nevertheless, it should be noticed that the dominant mechanism of the anisotropy evolves when ϕ increases. At ϕ close to ϕ_c, hardening of the emulsion in the direction normal to the pump is mostly responsible for the elastic anisotropy, while at larger ϕ values, the relative hardening is less pronounced, and the main source of anisotropy comes from softening parallel to the direction of the pump shear. Remembering that the origin of elasticity is different at ϕ close to ϕ_c and at higher values of ϕ, at volume fractions close to ϕ_c, there is a free volume in which the droplets can move without deforming, which facilitates the transfer of anisotropy of the structure from the direction of flow to the direction normal to the pump deformation. Remarkably, both mechanisms (softening parallel to the pump and hardening along the normal direction) lead to similar values of the eccentricity, at a given value of γ_π.

2.2 Fatigue protocol

We now consider cycling loading : the sample is submitted to a periodic deformation at frequency 10 Hz and of varying amplitude. At the end of the cycle of deformations, the sample is brought back to zero macroscopic deformation. The elastic response obeys to the same overall description as of the yield protocol (Fig. 3 **(c)**): a hardening in the perpendicular direction and a softening in the parallel direction, after a maximum value has been reached. Then, the parallel modulus reaches an asymptotic value, that is ≈ 10 % lower than

the modulus at rest. Similarly, in the normal direction, the system stiffens, and the modulus increases by ≈ 10 %. The overall value of the anisotropy is of the same magnitude than the value measured during the yield protocol, and the eccentricity, as measured at large γ_π values, is comprised between 0.4 and 0.5 (Fig. 3 **(d)**).

The appearance of anisotropy nevertheless differs between the yield and the fatigue protocols. The maximum of the elastic modulus in the $\parallel$ direction occurs at smaller γ_π strains than in the yield protocol (Fig. 4 **(a)**), and γ_π initially decays from 5 to 2.5 % when the volume fraction is comprised between ϕ_c and ϕ_{rcp}, and does not depend with the volume fraction for $\phi > \phi_{\text{rcp}}$. Conversely, in the fatigue protocol, γ_π^{max} increases continuously with ϕ and is close to the yield strain, as measured by standard rheology. Varying the number of pump cycles from 1 to 50 during the fatigue protocol does not affect the results. The main difference between the yield and the fatigue protocols thus lies in the fact that one comes back to the zero deformation state in the latter: particles rearrangements are triggered in both directions, and both contribute to the increase of $G_\parallel$, leading to higher $G_\parallel$ values in the fatigue than in the yield protocol (Fig. 4 **(a)** insert).

Moreover, the mechanisms of build-up of anisotropy differ, if one considers the eccentricity e as a function of ϕ (Fig. 4 **(b)**): whereas following the yield protocol, the contribution of hardening in the $\perp$ direction (dominant at ϕ close to ϕ_c) and that of softening along the $\parallel$ direction (dominant at higher ϕ), lead to an eccentricity at high γ_π that does not depend on ϕ, in the fatigue protocol the amplitude of the hardening along the $\perp$ direction depends weakly on the volume fraction, so that the eccentricity decreases with ϕ.

Conclusion

We have shown that the application of deformation leads to the appearance of persistent mechanical anisotropy in the emulsion. For pump amplitudes below the yield strain deformation, the suspension becomes stiffer in all directions, but for larger pump amplitudes, a strong modulus anisotropy develops : the emulsion is softer in the pump direction and stiffer in the direction normal to the pump. This general mechanism for generating mechanical anisotropy holds across all volume fractions and pump shear protocols. However the relative contributions of softening and hardening vary depending on whether elasticity primarily arises from packing constraints and entropic effects at lower ϕ, or from droplet deformations at higher ϕ.

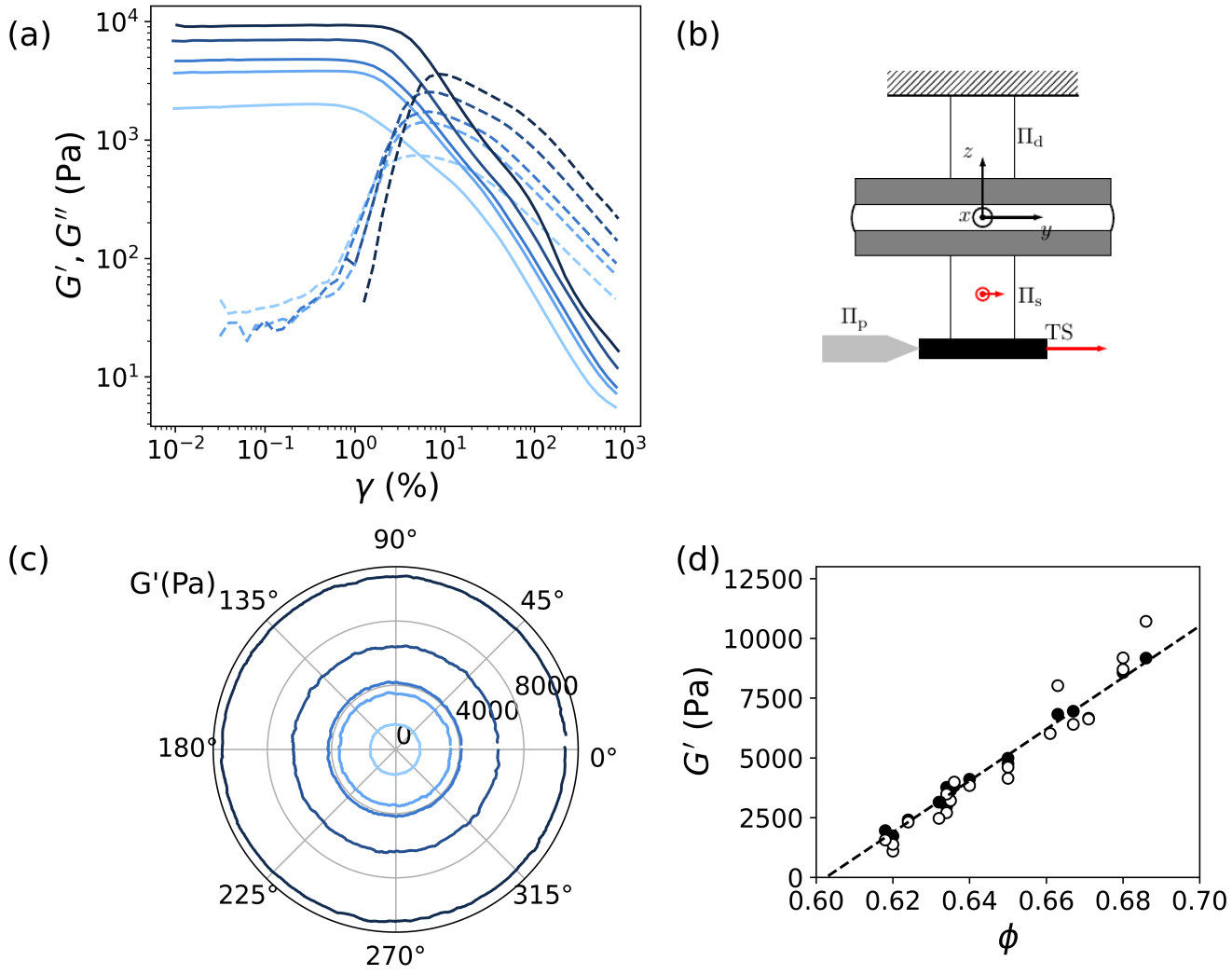

Fig. 1 (a) Elastic G' (continuous lines) and loss G'' (dashed lines) moduli of the concentrated suspensions, of volume fractions, $\phi = 0.618$, 0.634, 0.650, 0.667 and 0.686 (from light to dark blue) as a function of the shear amplitude γ, at frequency 10 Hz, measured by oscillatory rheology in cone/plate geometry (radius 12.5 mm and angle $2°$). A selection of measured volume fractions is represented. (b) PPMS (Pump Probe Mechanical Spectroscopy) setup : the sample is placed between two parallel disks, D_1 and D_2, separated by a 100 μm gap. The piezoelectric actuator Π_s applies shear in any direction of the xOy plane, with amplitude from 50 nm to 5 μm (0.05 % to 5 % shear). The stress components σ_{zx} ($\sigma_\perp$) and σ_{yz} ($\sigma_\parallel$) are measured by the piezoelectric actuator Π_d. The setup's bottom part is on a translation stage TS, enabling up to 60 % shear and defining the parallel (y) and normal (x) directions. (c) PPMS measurements of emulsion elastic moduli from (a), without pre-shear, at 10 Hz and 0.3 % amplitude. The angle denotes the difference between y and probe shear directions. (d). Elastic moduli in the linear regime versus emulsion concentration ϕ, measured by standard rheology (filled circles) and PPMS setup (empty circles).

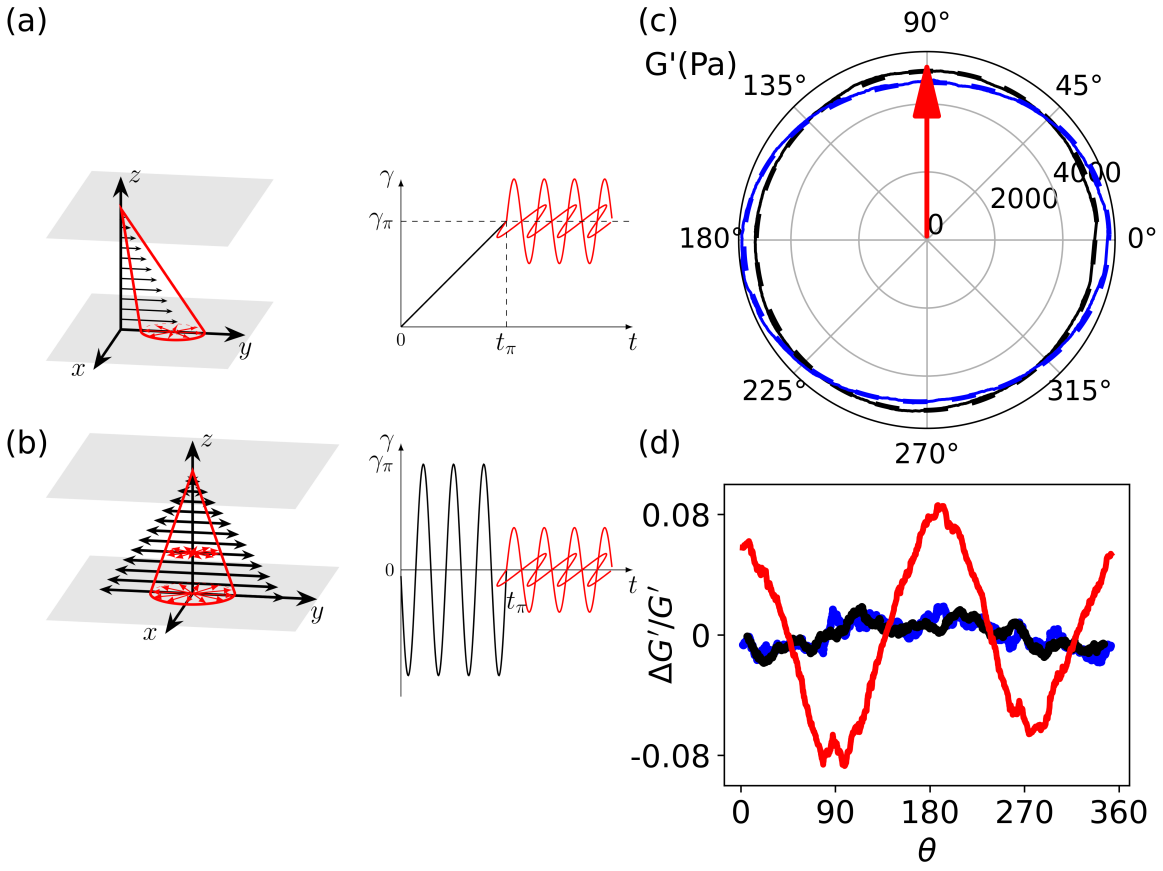

Fig. 2 Shear fields and their time dependence for the *yield* (a) and the *fatigue* (b) protocols. Black : pump shear and red : probe shear (not to scale). The sample is located between the two grey planes. The evolution of the strain as a function of time is also represented : γ_π is the amplitude of the pump shear and t_π its duration. (c) Typical angular dependence of the elastic modulus for $\phi = 0.645$ emulsion under $\gamma_\pi = 55$ % fatigue shear. Red arrow shows pump shear direction; black and blue data are moduli before and after pump shear. Dashed lines are ellipsoid fits. (d) Red line : relative difference between the elastic moduli after and before the application of the pump shear (same data as in (c)). The black and blue curves are the errors of the ellipse adjustments drawn in (c), before (black) and after (blue) the application of the pump shear.

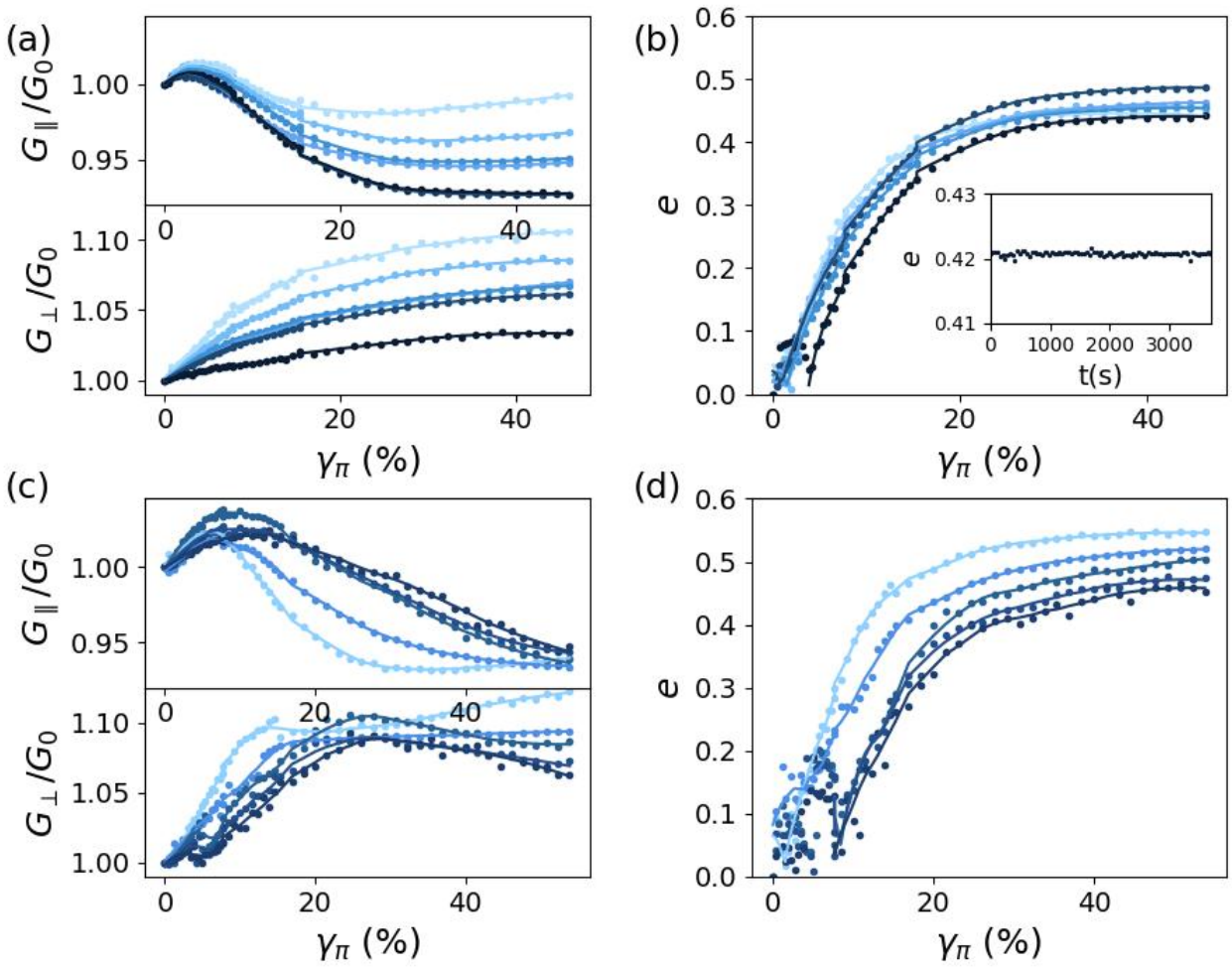

Fig. 3 (a) Elastic modulus parallel to the pump direction $G_\parallel$ and normal to the the pump direction $G_\perp$ as a function of the pump amplitude, γ_π, for a shear probe of frequency 10 Hz and amplitude 0.3 %, for the yield protocol (a) for emulsions of concentrations $\phi = 0.625,\ 0.636,\ 0.639,\ 0.650,\ 0.675$ and 0.70. (b) Eccentricity e of the elastic modulus as a function of the pump amplitude γ_π, corresponding to data represented in (a). *Insert* Evolution with time of the eccentricity for the emulsion of concentration $\phi = 0.70$ after the application of the yield pump protocol of amplitude 45 %. (c) and (d) Same quantities as for (a) and (b) obtained for the fatigue protocol, and for volume fractions $\phi = 0.63,\ 0.651,\ 0.67,\ 0.682$ and 0.701. In all figures, volume fractions increase from light blue to dark blue.

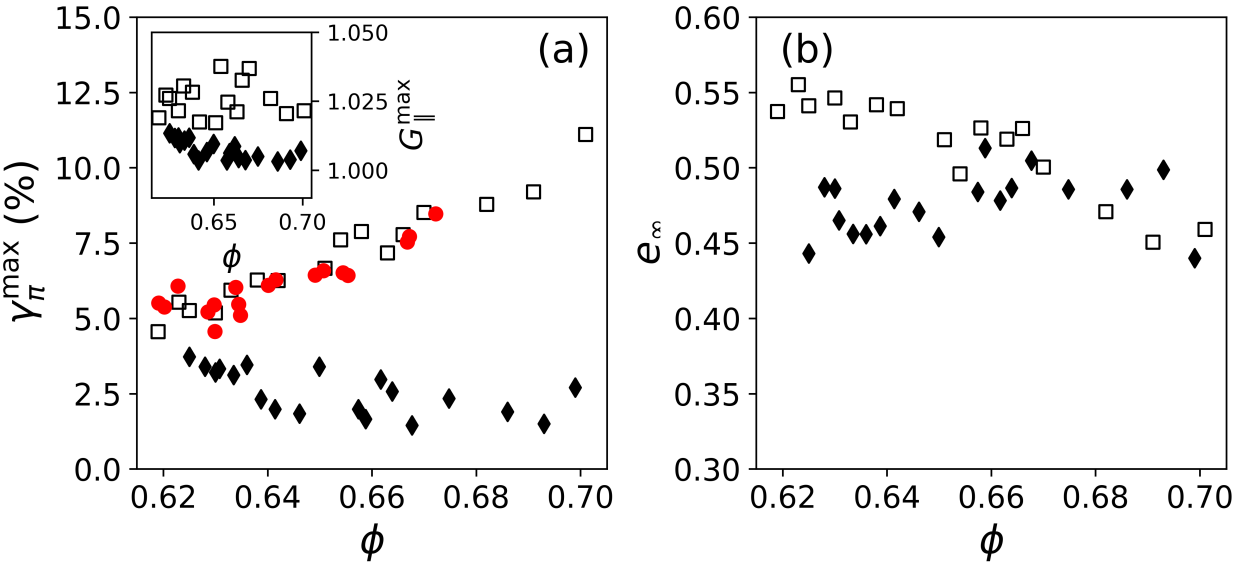

Fig. 4 (a) Pump amplitude at the maximum of $G_{\parallel}$, $\gamma_\pi^{\max}$, for the yield protocol (filled diamond), and for the fatigue protocol (empty squares), as a function of the volume fraction. The yield strain value is also reported (red disks). *Insert* : $G_{\parallel}$ values at $\gamma_\pi^{\max}$ for the yield (filled diamonds) and the fatigue (empty squares) protocols. (b) Evolution of the maximum eccentricity e_∞ (at large pump amplitudes) as a function of the emulsions concentration. Filled diamonds : yield protocol. Empty squares: fatigue protocol.

Conflicts of interest

There are no conflicts to declare.

Data availability

The data supporting this article have been included as part of the Supplementary Information.

Acknowledgements

The authors express their gratitude to B.Michel for assistance with the electronic control of the setup and to W.Grange for insightful discussions.

Notes and references

1 J. Dubliner, *Plasticity Theory*, Dover, 2008.

2 E. Nadgornyi, *Progress in Materials Science*, 1988, **31**, 1–530.

3 A. Argon, *Acta Metallurgica*, 1979, **27**, 47–58.

4 A. Argon, H.Y.and Kuo, *Proceedings of the Royal Society A*, 1979, **39**, 101–109.

5 M. Falk and J. Langer, *Physical Review >E*, 1998, **57**, 7192.

6 S. Suresh, *Fatigue of Materials*, Cambridge University Press, 1998.

7 L. Laursson and M. Alava, *Physical Review Letters*, 2012, **109**, 155504.

8 S. Karmakar, E. Lerner, I. Zylberg and J., *Physical Review E*, 2010, **82**, 031301.

9 D. Kushnir, C. Ruscher, E. Bartsch, F. Thalmann and P. Hébraud, *Physical Review E*, 2022, **106**, 034611.

10 N. Keim, J. Paulsen, Z. Zeravcic, S. Sastry and S. Nagel, *Reviews of Modern Physics*, 2019, **91**, 035002.

11 F.-M. Acrivos and A., *Journal of Rheology*, 1980, **24**, 799–814.

12 D. Pine, J. Gollub, L. A.M. and J.F.Brady, *Nature*, 2005, **438**, 997–1000.

13 L. Corté, P. Chaikin, J. Gollub and D. Pine, *Nature Physics*, 2008, **4**, 420–424.

14 D. Bi, J. Zhang, B. Chakraborty and R. Behringer, *Nature*, 2011, **480**, 355–358.

15 C.-P. Hsu, J. Mandal, S. Ramakrishna, N. Spencer and L. Isa, *Nature Communications*, 2021, **12**, 1477.

16 F. Ianni, D. Lasne, R. Sarcia and P. Hébraud, *Physical Review E*, 2006, **74**, 011401.

17 F. Spaepen, *Acta Metallurgica*, 1977, **25**, 407–415.

18 K. Jensen, D. Spaepen and F., *Physical Review E*, 2014, **90**, 042305.

19 G. Picard, A. Ajdari, F. Lequeux and L. Bocquet, *European Physical Journal E*, 2004, **15**, 371–381.

20 F. Blanc, F. Peters, J. Gillissen, M. Cates, S. Bosio, C. Benarroche and R. Mari, *Physical Review Letters*, 2023, **130**, 118202.

21 D. Bonn, M. Denn, L. Berthier, T. Manneville and S., *Review of Modern Physics*, 2017, **89**, 035005.

22 P. Hébraud, F. Lequeux and J.-F. Palierne, *Langmuir*, 2000, **16**, 8296–8299.

23 T. Athanasiou, G. Auernhammer, D. Petekidis and G., *Rheologica Acta*, 2019, **58**, 619–637.

24 B. Schroyen, D. Vlassopoulos, P. Van Puyvelde and J. Vermant, *Rheologica Acta*, 2020, **59**, 1–22.

25 T. Mason and D. Weitz, *Physical Review Letters*, 1995, **74**, 1250–1253.

26 H. Gang, A. Krall and D. Weitz, *Physical review E*, 1995, **52**, 6289.